The Dynamics of Flow Forced Distributed Parameter Heat Exchangers

F. J. STERMOLE and M. A. LARSON

Iowa State University, Ames, Iowa

The purpose of this investigation was to study the dynamics of concentric double pipe heat exchangers subjected to flow rate perturbations, with primary emphasis being given to countercurrent heat exchange. The approach presented in this paper utilizes frequency response analysis to test the hypothesis that a heat exchanger can be treated as a linear system when subjected to flow disturbances. The heat exchange results obtained in this investigation are representative of a wide range of distributed parameter processes and form the basis for study of the more complicated processes.

Previous work done on flow rate upsets in double pipe concentric tube heat exchangers is limited. Mozley (5) presented one of the first lumped parameter representations of double pipe heat exchangers to appear in the literature but did not give experimental verification for flow rate upsets. Hempel (3) derived transfer function models of a steam-water heat exchange system for flow upsets as well as temperature upsets and included the effects of wall capacitance and heat transfer coefficient variation. Comparison of experimental and theoretical frequency response results was good, and resonance was predicted. Stermole and Larson (7) presented both lumped and distributed parameter models for steam-water exchangers and obtained good agreement between experimental and theoretical frequency response results when wall capacitance and heat transfer coefficient variation were neglected. Koppel (4) obtained a model for the flow upset dynamics of a steam-water heat exchanger by applying the method of characteristic equations to a partial differential equation representation of the system. Edwards' dissertation (1) contains a treatment of the derivation of flow forced transfer functions in compact matrix notation for digital computer analysis of a countercurrent heat exchanger. Comparison of theoretical and experimental results was good, but the effect of resonance was not observed experimentally nor predicted theoretically.

MATHEMATICAL DEVELOPMENT

A mathematical description of a distributed parameter double pipe heat exchanger with fluid flowing in both the shell and tube may be obtained from heat balances over both fluid phases and the metal wall. The resulting equations for countercurrent heat exchange are

$$\frac{\partial \theta_s}{\partial t} = V_s \frac{\partial \theta_s}{\partial x} = \frac{h_s P_s}{\rho_s A_s C p_s} (\theta_w - \theta_s) \qquad (1)$$

$$\frac{\partial \theta_t}{\partial t} + V_t \frac{\partial \theta_t}{\partial x} = \frac{h_t P_t}{\rho_t A_t C p_t} (\theta_w - \theta_t) \qquad (2)$$

$$\frac{\partial \theta_w}{\partial t} = \frac{h_s P_s}{\rho_w A_w C p_w} (\theta_s - \theta_w) + \frac{h_t P_t}{\rho_s A_s C p_s} (\theta_t - \theta_w) \qquad (3)$$

These equations are based on the usual assumptions (7). The direction of flow of tube fluid has been taken in the same direction as the coordinate system. These equations are identical to those that describe a concurrent flow heat exchanger except for the negative sign on the term involving V_s in Equation (1). This makes application of the boundary conditions more complicated for countercurrent than for concurrent flow.

Starting with Equations (1), (2), and (3) several mathematical models have been developed to relate output tube fluid temperature to shell and tube flow rate upsets. Development of these models was directed toward studying the effects of tube wall capacitance, heat transfer coefficient variation, and lumped parameter representation of the distributed parameter system in an effort to satisfactorily represent the flow forced heat exchange system with the simplest model possible. Both transient and frequency response to flow rate upsets were used to test the models against experimental data.

The derivation is presented for upsets in either the shell or tube flow rate in a form that permits obtaining transfer functions for either V_t or V_s forcing θ_t. The transfer functions presented in this paper are approximate models obtained by neglecting appropriate temperature forcing terms that increase the complexity of a theoretical description of the system but contribute little to its accuracy.

For flow rate disturbances Equation (1), (2), and (3) are linear but must be reduced to constant coefficient equations to permit application of standard Laplace transformation techniques to obtain desired transfer functions with the technique presented in previous papers (3, 6, 7). This is accomplished by letting θ_t, θ_s, and θ_w and the coefficients V_t, V_s, B_t, B_s, B_3, and B_4 be expressed as the sum of a steady state value and a perturbation from steady state.

Substitution into Equations (1), (2), and (3) and dropping the terms involving the product of two perturbations one gets the equations in terms of steady state and dynamic quantities. Subtraction of the steady state equations from the total equations yields dynamic equations. The resulting equations are linear and have constant coefficients with respect to time on all forcing and dependent variables. Laplace transformation of these equations with respect to time and combination of the resulting equations to eliminate wall temperature yields

$$\frac{d\bar{\theta}_s}{dx} - a_1\bar{\theta}_s = g_1\bar{V}_t + h_1\bar{V}_t e^{m_1 x} - f_1\bar{\theta}_t \qquad (4)$$

$$\frac{d\bar{\theta}_t}{dx} + a_2\bar{\theta}_t = g_2 V_t + h_2\bar{V}_t e^{m_1 x} + f_2\bar{\theta}_s \qquad (5)$$

Equations (4) and (5) may be solved for transfer functions involving tube temperature forced by either shell or tube flow rate upsets with the countercurrent boundary conditions $\bar{\theta}_s = 0$ at $x = L$ and $\bar{\theta}_t = 0$ at $x = 0$ since the input shell and tube temperatures are constant. However the resulting transfer functions are extremely long and complex and of questionable practical value. In an effort to obtain the transfer function $\bar{\theta}_t/\bar{V}_t$ in a more useable form the significance of each term in Equation (5) was investigated. Temperature of the tube fluid is being forced by the change in flow rate of the tube fluid and by the

F. J. Stermole is at the Colorado School of Mines, Golden, Colorado.

temperature change of shell fluid. Comparison of the magnitude of these forcing terms with experimental data shows that for equal mass flow rates in the shell and tube the temperature forcing term is about 7% as large as the flow forcing terms. For mass flow rates in the shell greater than in the tube the effect of shell temperature change is proportionately less until at infinite shell flow rates the shell temperature remains constant and contributes nothing to the dynamics of flow upsets. The infinite shell flow rate case is analogous to a steam jacketed heat exchanger in that shell temperature remains constant. For all these cases when tube flow upsets occur the change in residence time of the tube fluid and heat transfer coefficient variation are more important considerations than changes in shell temperature. This is expected if one considers the source of the shell temperature forcing term in Equation (5). An upset in V_t causes a change in θ_t and the heat transfer coefficient which causes θ_s to change. The change in θ_s reflects back to the tube causing another correction in θ_t which is always small compared with the original temperature change. Neglecting the temperature forcing term involving $\bar{\theta}_s$ in Equation (5) one obtains the following transfer function:

$$\frac{\bar{\theta}_{tL}}{\bar{V}_t} = \frac{h_2}{m_1 + a_2}\left(a^{m_1 L} - e^{-a_2 L}\right) + \frac{g_2}{a_2}\left(1 - e^{-a_2 L}\right)$$

Model I

The g_2 is directly dependent upon heat transfer coefficient variation. With reference to the defining equation for g_2, if the tube side heat transfer film coefficient is considered constant, $k_t = 0$ and therefore $g_2 = 0$. h_2 does not go to zero if the heat transfer coefficient is considered constant; therefore for constant heat transfer coefficients

$$\frac{\bar{\theta}_{tL}}{\bar{V}_t} = \frac{h_2}{m_2 + a_2}\left(e^{m_1 L} - e^{-a_2 L}\right) \qquad \text{Model II}$$

Similar models can be obtained for shell flow upsets by neglecting the temperature forcing term involving $\bar{\theta}_t$ in Equation (4).

If the tube wall capacitance is considered to be negligible, the left side of Equation (3) is equal to zero. Combining Equations (1), (2), and (3) to eliminate the tube wall temperature one obtains the following two partial differential equations with an overall heat transfer coefficient:

$$\frac{\partial \theta_s}{\partial t} - V_s \frac{\partial \theta_s}{\partial x} = K_s\left(\theta_t - \theta_s\right) \tag{6}$$

$$\frac{\partial \theta_t}{\partial t} + V_t \frac{\partial \theta_t}{\partial x} = K_t\left(\theta_s - \theta_t\right) \tag{7}$$

Transfer functions for $\bar{\theta}_t/\bar{V}_t$ and $\bar{\theta}_t/\bar{V}_s$ can be derived from Equations (6) and (7) by utilizing the same procedure used to develop Model I. These same transfer functions can also be used to represent shell temperature forced by upsets in either flow rate by properly changing the subscript nomenclature, that is by interchanging shell and tube parameters and variables in the equations. The overall heat transfer coefficient is considered to vary directly with upsets in either fluid flow rate. The temperature and flow rate variables are expressed as the sum of steady state and perturbation values and are substituted into Equations (4) and (5). Dropping the products of perturbations, subtracting the steady state equations, and transforming one gets the following equations:

$$\frac{d\bar{\theta}_s}{dx} - \alpha_1 \bar{\theta}_s = -\frac{K_{si}}{V_{si}}\bar{\theta}_t - N_1 e^{m_2 x}\bar{V}_s - K_{si}\left(C + De^{m_2 x}\right)\left(\frac{k_s \bar{V}_s}{V_{si}} + \frac{k_t \bar{V}_t}{V_{ti}}\right) \tag{8}$$

$$\frac{d\bar{\theta}_t}{dx} + \alpha_2 \bar{\theta}_t = \frac{K_{ti}}{V_{ti}}\bar{\theta}_s - N_2 e^{m_2 x} V'_t - K_{ti}\left(C + De^{m_2 x}\right)\left(\frac{k_s \bar{V}_s}{V_{si}} + \frac{k_t \bar{V}_t}{V_{ti}}\right) \tag{9}$$

Tube Flow Upset

When one neglects the temperature forcing term involving $\bar{\theta}_s$ in Equation (9), the following transfer function is obtained for tube flow rate forcing tube temperature with a constant shell flow rate:

$$\frac{\bar{\theta}_{tL}}{\bar{V}_t} = -\frac{(N_2 + R_2)}{m_2 + \alpha_2}\left(e^{m_2 L} - e^{-\alpha_2 L}\right) - \frac{Q_2}{\alpha_2}\left(1 - e^{-\alpha_2 L}\right)$$

Model III

For a constant overall heat transfer coefficient R_2 and Q_2 are zero because $k_t = 0$. Therefore the model that results when a constant overall heat transfer coefficient is assumed is as follows:

$$\frac{\bar{\theta}_{tL}}{\bar{V}_t} = -\frac{N_2}{m_2 + \alpha_2}\left(e^{m_2 L} - e^{-\alpha_2 L}\right) \qquad \text{Model IV}$$

For equal mass flow rates in the shell and tube $m_2 = 0$, and Model IV reduces to

$$\frac{\bar{\theta}_{tL}}{\bar{V}_t} = \frac{-N_2}{\alpha_2}\left(1 - e^{-\alpha_2 L}\right) \tag{10}$$

For infinite shell flow rate (constant shell temperature) $m_2 = -K_{ti}/V_{ti}$ since $K_{si}/V_{si} = 0$. Therefore for an infinite shell flow rate Model IV reduces to the same transfer function that is obtained for a steam-water heat exchanger forced by flow rate upsets as presented by Stermole and Larson (7):

$$\frac{\bar{\theta}_{tL}}{\bar{V}_t} = \frac{-N_2 V_{ti}}{s} e^{-\frac{K_{ti} L}{V_{ti}}\left(1 - e^{-\frac{sL}{V_{ti}}}\right)}$$

Models III and IV can be made applicable to concurrent heat exchange by changing the sign of V_{si}, which appears only in m_2. This yields a different limiting model for equal mass flow rates than the countercurrent model because m_2 does not go to zero. It should be noted that these models for tube flow upsets are identical for concurrent and countercurrent heat exchange except for the sign of V_{si} because a boundary condition on shell fluid was not used in their derivation. The transfer functions for shell flow upsets forcing tube temperatures are not interchangeable in this simple manner for concurrent and countercurrent exchangers because boundary conditions on both fluids are needed for this derivation, and therefore each model is different.

In summary, Models III and IV are applicable to countercurrent, concurrent, and constant shell temperature heat exchange when the correct value of m_2 is used for each case. Other parameters are the same for all cases. The differences in m_2 are summarized as follows:

Countercurrent, unequal mass flow rates, $m_2 = \frac{K_{si}}{V_{si}} - \frac{K_{ti}}{V_{ti}}$

Countercurrent, equal mass flow rates, $m_2 = 0$

Concurrent, unequal mass flow rates, $m_2 = -\frac{K_{si}}{V_{si}} - \frac{K_{ti}}{V_{ti}}$

Concurrent equal mass flow rates, $m_2 = -\frac{2K_{ti}}{V_{ti}}$

Constant shell temperature

(infinite shell flow), $m_2 = -\dfrac{K_{ti}}{V_{ti}}$

Shell Flow Upset

A transfer function for shell flow upsets forcing tube temperature can be obtained by neglecting the temperature forcing term involving $\bar{\theta}_t$ in Equation (8) and combining Equations (8) and (9) with the boundary conditions previously given. However a series approximation solution can be employed to obtain both $\bar{\theta}_t/\bar{V}_s$ and $\bar{\theta}_t/\bar{V}_t$. This method was used by Gilliland, Gould, and Rinard (*10*) for temperature upsets in a double pipe heat exchanger. It shows that keeping only the first term in the series representation of either $\bar{\theta}_t/\bar{V}_t$ or $\bar{\theta}_t/\bar{V}_s$ neglects the temperature forcing term in the equation for the fluid that is upset, and that in fact the same transfer functions result that are obtained by neglecting these temperature terms in Equation (8) and (9) and by using the derivation previously described. Note that while the approximation that results in Model IV is due to neglecting the $\bar{\theta}_s$ temperature forcing term in Equation (9), the approximation that yields the $\bar{\theta}_t/\bar{V}_s$ transfer function is due to neglecting the $\bar{\theta}_t$ temperature forcing term in Equation (8).

For a constant overall heat transfer coefficient Equations (8) and (9) are integrated individually with the boundary conditions $\bar{\theta}_{t0} = 0$ and $\bar{\theta}_{sL} = 0$. Following the general procedure previously presented (*10*) the resulting equations are combined to eliminate $\bar{\theta}_s$. This yields

$$\bar{\theta}_t = \frac{K_{ti}\,K_{si}}{V_{ti}\,V_{si}}\,e^{-\alpha_2 x}\int_o^x e^{(\alpha_1+\alpha_2)x_2}\left[\int_{x_2}^L e^{-\alpha_1 x_1}\,\bar{\theta}_t\,dx_1\right]dx_2$$

$$+\frac{K_{ti}}{V_{ti}}N_1\,e^{-\alpha_2 x}\int_o^x e^{(\alpha_1+\alpha_2)x_2}\left[\int_{x_2}^L e^{(m_2-\alpha_1)x_1}\bar{V}_s\,dx_1\right]dx_2$$

$$-N_2\,e^{-\alpha_2 x}\int_o^x e^{(m_2-\alpha_2)x_1}\,\bar{V}_t\,dx_1 \qquad (12)$$

Define the integral operator $I\,(\bar{\theta}_t)$ as

$$I\,(\bar{\theta}_t) = \frac{K_{ti}\,K_{si}}{V_{ti}\,V_{si}}\,e^{-\alpha_2 x}\int_o^x e^{(\alpha_1+\alpha_2)x_2}\left[\int_{x_2}^L e^{-\alpha_1 x}\bar{\theta}_t\,dx_1\right]dx_2$$

Let the function $f\,(x, s)$ be

$$f\,(x_1 s) = \frac{K_{ti}\,N_1}{V_{ti}}\,e^{-\alpha_2 x}\int_o^x e^{(\alpha_1+\alpha_2)x_2}$$

$$\left[\int_x^L e^{(m_2-\alpha_1)x_1}\,\bar{V}_1\,dx_1\right]dx_2 - N_2\,e^{-\alpha_2 x}\int_o^x e^{(m_2+\alpha_2)x}\,\bar{V}_2 dx$$

Equation (12) may now be written as

$$\bar{\theta}_t = I\,(\bar{\theta}_t) + f\,(x, s)$$

Solving for $\bar{\theta}_t$ one gets $\bar{\theta}_t = \dfrac{f(x, s)}{1 - I}$. The right side of Equation (7) may be expanded in a series to give

$$\bar{\theta}_t = \sum_{n=o}^{\infty} I^n\,\{f(x, s)\}$$

where I^n means that the operation I is applied n times.

For $n = 0$ it is easily seen that $\bar{\theta}_t = f(x, s)$, and therefore the double integral of $\bar{\theta}_t$ is neglected in the one-term approximation. Going back to the origin of Equation (12), it may be seen that this double integral term represents the change in $\bar{\theta}_t$ caused by the interaction between $\bar{\theta}_t$ and $\bar{\theta}_s$ when an upset occurs. This is the effect that is neglected in the one-term approximation of $\bar{\theta}_t/\bar{V}_t$ which yields Model IV. Consideration of higher-order terms in the series will account for the effect of higher-order temperature reflections between the shell and tube.

For an upset in V_s a change in θ_s results which causes a corresponding change in θ_t. This change in θ_t reflects back to the shell causing further change in θ_s which then causes more change in θ_t. It is this latter temperature reflection that is neglected in the first-term approximation of $\bar{\theta}_t/\bar{V}_s$ which is as follows:

$$\frac{\bar{\theta}_{tL}}{\bar{V}_s} = \frac{K_{ti}\,N_1\,e^{m_2 L}}{V_{ti}\,(m_2-\alpha_1)\,(\alpha_1+\alpha_2)}\,(1 - e^{-(\alpha_1+\alpha_2)L})$$

$$-\frac{K_{ti}\,N_i}{V_{ti}\,(m_2-\alpha_1)\,(m_2+\alpha_2)}\,(e^{m_2 L} - e^{-\alpha_2 L}) \qquad \text{Model V}$$

To use the partial differential equation transfer function Models I through V to predict transient response, it is necessary to invert the equations to real time and solve for θ_{tL} by substituting different values of time into the equation. However it is known that the final temperature predicted is very strongly dependent upon heat transfer coefficient variation with flow changes, so only Models I and III which account for the effect of heat transfer coefficient variation can be expected to predict accurate transient response curves. These models predict good transient response results for small flow upsets but give poor results for large flow upsets. This is due to the dropping of terms involving products of perturbations when Equations (6) and (7) are reduced to constant coefficient equations.

EXPERIMENTAL INVESTIGATION

A double pipe heat exchanger was constructed that could be operated as a concurrent, countercurrent, or steam-water heat exchange system with only minor changes in the piping system. A flow sheet of the countercurrent system used in this investigation is shown in Figure 1. The heat exchanger was constructed with a 1 in. nominal type K copper tube concentrically mounted inside a 2 in. nominal schedule 40 iron pipe shell. The exchanger was 14.7 ft. long from the center line of the shell input to center line of the shell output. The shell was insulated with ¾-in. Fiberglass pipe insulation. Hot water flowed through the tube from the constant head tank and was cooled by countercurrent cold water flowing in the shell. Steam injected into water flowing into the constant head tank produced the hot water. The heated water was discharged into an elevated 55 gal. holdup tank at a flow rate great enough to always maintain an overflow. This provided a constant temperature and constant pressure hot water source.

A series thermocouple with seven probes constructed of 24 gauge copper-constantan wire was placed in the outlet tube stream to provide a continuous temperature signal to d.c. amplifier-recorder equipment. The time constant of the thermopile

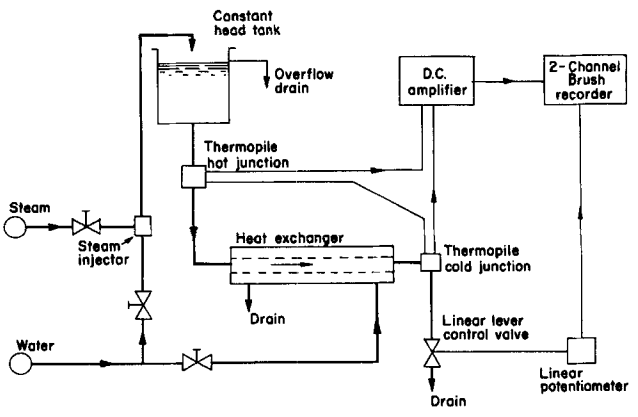

Fig. 1. Flow diagram of countercurrent heat exchange system.

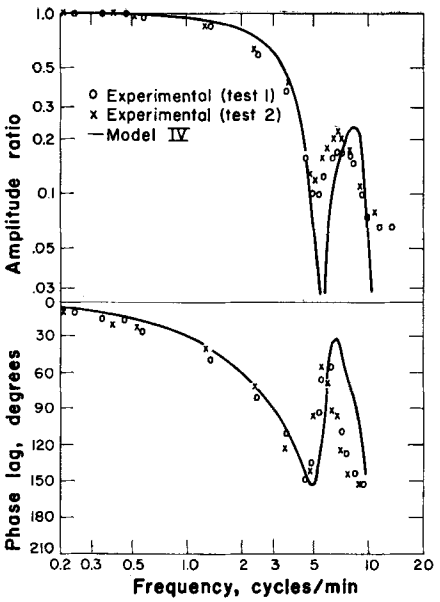

Fig. 2. Experimental frequency response for tests 1 and 2, and theoretical frequency response obtained with Model IV.

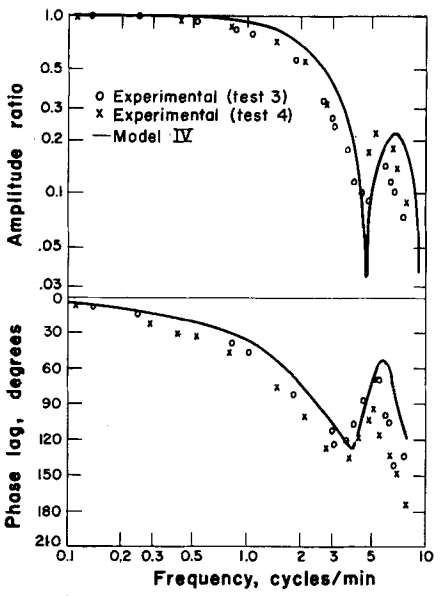

Fig. 3. Experimental frequency response for tests 3 and 4, and theoretical frequency response obtained with Model IV.

was about one-tenth of a second. The thermopile was mounted in a long probe so that it could be inserted into the end of the heat exchanger such that measurement of the temperature of tube fluid at the center line of entering shell fluid could be effected. This eliminated temperature measurement transport lag. Continuous recording of changes in flow rate was made possible by a linear sliding arm potentiometer in series with a 1½-v. d.c. battery. The sliding arm of the potentiometer was spring loaded against the lever of the flow control valve and thus continuously converted the valve position into an electrical signal which was recorded on one channel of a two channel stripchart recorder. Temperature response from the thermopile signal was recorded on the second recorder channel after the thermopile signal had been amplified by a high gain d.c. amplifier. This side by side recording of the input flow forcing signal and the output temperature response signal made it very convenient to obtain magnitude ratio and phase lag information from frequency response data.

Six tests were made at various flow conditions. Each test consisted of taking both transient and frequency response data over the same flow range. Resonance was observed for each of the six frequency response tests and was found to be a function only of heat exchanger length (L), upset frequency of either fluid (ω), and velocity of the fluid (V) whose temperature was being measured (not necessarily the fluid being upset). For all tests resonance occurred when $L\omega/V = 2\pi$, where the resonance frequency is defined as the frequency at which the amplitude ratio ceases to attenuate and starts to get larger. Tests 1 and 2 with unequal mass flow rates in the shell and tube were made to see if any difference could be observed between frequency response results for large and small tube flow changes about the same mean flow rate. Tests 1 and 2 had respective tube flow upsets of 48 and 21% of a 28.2 lb./min. mean flow rate. Tests 3 and 4 had respective tube flow upsets of 65 and 26% of a 23.0 lb./min. mean tube flow rate. Shell flow rate was equal to 210 lb./min. for Tests 1 and 2 but was equal to mean tube flow for Tests 3 and 4. The large flow changes did not give frequency response results significantly different from the small flow changes as may be seen in Figures 2 and 3. Transient response data were measured over the same flow ranges for which frequency response data were taken. Sample test conditions and steady state data are given in Table 1.

Table 1. Sample Steady State Data for the Maximum and Minimum Flow Rates of Two Countercurrent Experimental Frequency and Transient Response Tests

	lb./min.	θ_{s0i} (°F.)	θ_{sLi} (°F.)	θ_{t0i} (°F.)	θ_{tLi} (°F.)	U [B.t.u./(min.)(sq. ft./°F.)]
Test 1 (tube flow upset)						
Wmax	35.0	66.2	59.0	153.5	110.0	5.85
Wmin	21.5	64.2	59.0	153.5	102.5	4.46
Wshell	210					
Test 5 (shell flow upset)						
Wmax	66.0	75.0	59.0	164.0	125.5	3.44
Wmin	27.0	85.7	59.0	164.0	136.0	2.42
Wtube	26.0					

Test 5 was conducted for shell flow upsets forcing output tube temperature to see if shell flow upsets gave any notable differences in the frequency and transient response curves from the tube flow upsets of Tests 1 to 4. Frequency response data of Test 5 are plotted in Figure 6 and are generally similar to the tube flow upset data. For shell flow upsets the tube fluid temperature resonance frequency was found to be a function only of the tube flow rate, and the frequency at which resonance occurs is readily predictable from $L\omega/V = 2\pi$, where V is the velocity of tube flow rate. For the conditions of Test 5 shell temperature response resonance would be at a much different frequency than the tube resonance because average shell fluid velocity is only about one-half the tube fluid velocity. This would cause shell resonance to occur at a frequency about one-half as great as the tube resonance frequency.

DISCUSSION

The frequency response results for Test 1 through 6 show that resonance is a very dominant factor in determining the shape of frequency response curves for this system. The term resonance is used here to mean the change from a decreasing to an increasing amplitude ratio with increasing upset frequency. Resonance frequency refers to the frequency at which the amplitude ratio ceases to attenuate and starts to get larger with increasing frequency.

Resonance occurs in distributed parameter heat exchangers because of variation in the length of time an element of fluid takes to pass through the shell or tube of a heat exchanger. For two fluid flow each fluid has its own independent resonance frequency. For illustrative pur-

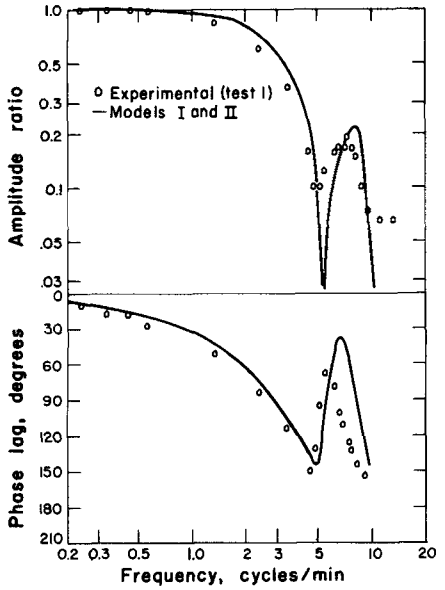

Fig. 4. Experimental frequency response for test 1 and theoretical frequency response obtained with Models I and II.

poses consider a tube flow upset forcing tube temperature with a constant shell temperature. At steady state all elements of tube fluid have the same residence time in the exchanger. When flow rate is pulsed sinusoidally at low frequencies, some elements of fluid enter the exchanger at maximum flow rate and require less time to pass through the exchanger than those that enter at minimum flow rate. Thus some elements of fluid are heated more than others, and a periodic temperature response curve results. As upset frequency is increased, the response curve attenuates because the average residence time of an element of fluid that entered the exchanger at maximum flow rate becomes larger and the residence time becomes smaller for the fluid element entering at minimum flow rate. The resonance frequency occurs when the upset frequency in cycles per unit time equals the reciprocal of the residence time of an element of fluid at the mean flow rate. At the resonance frequency each element of fluid requires the same length of time to pass through the heat exchanger, regardless of whether it enters the exchanger at maximum, minimum, or average flow rate. Therefore for tube flow upsets forcing tube temperature at the resonance frequency the temperature response curve would be a straight line (zero amplitude ratio) if a perfect sinusoidal flow upset was being impressed upon the system and if the variations in temperature driving force and heat transfer coefficient along the length of the heat exchanger were a negligible consideration. Increasing the frequency above the resonance frequency again causes a variation in the residence time of fluid flowing through the tube, and consequently an increase in temperature amplitude occurs. Increasing the upset frequency further again causes attenuation.

The frequency response results for tube, shell, and simultaneous tube and shell flow upsets verify that resonance depends upon the L/V ratio of the fluid whose temperature is being measured and that resonance occurs when $L\omega/V = 2\pi$ with ω expressed in radians per second. This is also predicted by any of the appropriate partial differential equation Models I to V. Wall capacitance and heat transfer coefficient variation do not effect the resonance frequency. In each of Models I to V the transport delay term $e^{-iL\omega/V}$ appears. This can be written as Cos $L\omega/V - i$ sin $L\omega/V$. The sine and cosine terms repeat themselves at every multiple of 2π which is the factor which causes resonance to be predicted when $L/V = 2\pi$ or integral multiples of 2π. The same transport term exists in the models for steam temperature upsets previously reported (7). If the temperature reflections of higher-order terms in the series approximation solution are considered, transport delay terms appear that would predict resonance at a different frequency, but these terms are always small compared with the $e^{-iL\omega/V}$ transport term and the latter term dominates.

In Figures 2 and 3 it may be observed that the magnitude of flow rate perturbations had no significant effect on normalized frequency response results in the range of flow upsets studied, and that Model IV, which was developed from partial differential equations neglecting wall capacitance and heat transfer coefficients variation, gives good agreement with experimental data. Theoretical frequency response results do not depend upon the upset magnitude because normalizing the amplitude ratios eliminates the effect of perturbation size, so the same theoretical curve results for both Tests 1 and 2.

In Figures 4 and 5 the data of Test 1 and Test 3 were checked with Models I and II to observe the effect of wall

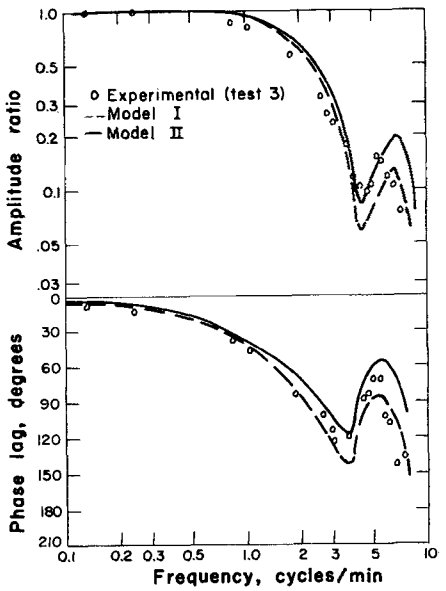

Fig. 5. Experimental frequency response for test 3, and theoretical frequency response obtained with Models I and II.

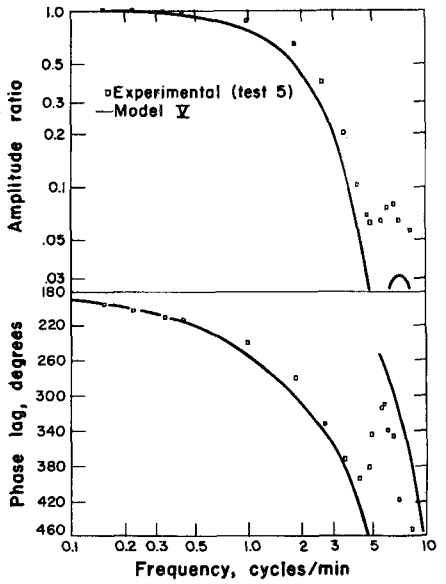

Fig. 6. Experimental frequency response for test 5, and theoretical frequency response obtained with Model V.

capacitance and heat transfer coefficient variation. Figure 4 shows that for Test 1 with a large shell flow identical theoretical results are obtained with Model I which includes heat transfer film coefficient variation and with Model II which neglects it. These theoretical results are in turn nearly identical with the results of Model IV. This indicates that for a nearly constant shell temperature (high flow rate or steam in shell) heat transfer coefficient variation and wall capacitance have a negligible effect on normalized frequency response results. Figure 5 shows that for equal flow rates in the shell and tube a slight improvement resulted by including the heat transfer coefficient variation in Model I. Whether the added work of calculating the extra term in Model I is worth the slight improvement in results is questionable.

Comparing the results of Figures 3 and 5 shows that including the effect of wall capacitance softens the resonance frequency dip. Neglecting the heat transfer coefficient variation makes the dip even softer. Including the wall capacitance also gives a slight improvement to phase lag results.

Figure 6 shows that shell flow upset data of Test 5 are in relatively good agreement with Model V. Phase lag agreement is excellent over the full range of frequencies tested. The resonance frequency dip does not go to zero but is very small.

Transient response data for small flow upsets give fairly good agreement with the predictions of Model III. Results obtained when Model III was compared with the transient data of Tests 1 and 3 for large flow upsets were very poor. Final temperatures predicted were in error by 50 to 75%. This is due to dropping the product of perturbation terms in reducing the partial differential equations to constant coefficient equations. For large upsets the product of perturbation terms may be as large as the steady state terms, and neglecting them introduces significant error into final temperatures predicted. Frequency response results are not effected however because the effect of perturbation magnitude is eliminated by normalizing the amplitude ratio.

In summary the approximate transfer functions presented in this paper give a good representation of the dynamics of the system. The Models I to V predict correct final value temperatures for small transient upsets and give good frequency response results for both large and small upsets. Resonance is predicted and is shown to be a characteristic of distributed parameter systems, occurring in each fluid at the frequency determined by the residence time of the fluid passing through the system.

ACKNOWLEDGMENT

This investigation was supported by the Iowa Engineering Experiment Station.

NOTATION

A = cross-sectional area, sq. ft.
Cp = heat capacity, B.t.u./(lb.)(°F.)
h_t, h_s = heat transfer film coefficient, B.t.u./(sec.)(sq. ft./°F.)
k = dimensionless constant relating flow changes to heat transfer coefficient changes
L = heat exchanger length, ft.
P_s = outside perimeter of tube, ft.
P_t = inside perimeter of tube, ft.
p = Laplace transform operator for length, ft.$^{-1}$
s = Laplace transform operator for time, sec.$^{-1}$
t = time, sec.
U = overall heat transfer coefficient, B.t.u./(sec.)(sq. ft./°F.)
V = fluid velocity, ft./sec.
W = mass flow rate, lb./min.
x = axial distance coordinate, ft.
ρ = density, lb./cu. ft.
θ = temperature, °F.
ω = frequency, cycles/min. or rad./sec.

Subscripts

i = initial steady state value
L = at axial distance $x = L$
0 = at axial distance $x = 0$
s = refers to shell or fluid in shell
t = refers to tube or fluid in tube
w = tube wall

Superscripts

$'$ = deviation from initial steady state value
$\bar{\ }$ = Laplace transformed variable with respect to time

Grouped Coefficients

$$a_1 = \frac{(s + B_{si})(s + B_{3i} + B_{4i}) - B_{si}B_{3i}}{V_{si}(s + B_{3i} + B_{4i})}$$

$$a_2 = \frac{(s + B_{ti})(s + B_{3i} + B_{4i}) - B_{ti}B_{4i}}{V_{ti}(s + B_{3i} + B_{4i})}$$

$$B_s = \frac{h_s P_s}{\rho_s A_s Cp_s} = B_{si}\left(1 + \frac{k_s V_s'}{V_{si}}\right)$$

$$B_t = \frac{h_t P_t}{\rho_t A_t Cp_t} = B_{ti}\left(1 + \frac{k_t V_t'}{V_{ti}}\right)$$

$$B_3 = \frac{h_t P_t}{\rho_w A_w Cp_w} = B_{3i}\left(1 + \frac{k_s V_s'}{V_{si}}\right)$$

$$B_4 = \frac{h_s P_s}{\rho_w A_w Cp_w} = B_{4i}\left(1 + \frac{k_t V_t'}{V_{ti}}\right)$$

$$C = \frac{(\theta_{t0i} - \theta_{s0i})\, e^{m_2 L} - (\theta_{tLi} - \theta_{sLi})}{e^{m_2 L} - 1}$$

$$D = \frac{\theta_{tLi} - \theta_{sLi} - \theta_{t0i} + \theta_{s0i}}{e^{m_2 L} - 1}$$

$$f_1 = \frac{B_{si}B_{4i}}{V_{si}(s + B_{3i} + B_{4i})}$$

$$f_2 = \frac{B_{ti}B_{3i}}{V_{ti}(s + B_{3i} + B_{4i})}$$

$$g_1 = \frac{B_{si}B_{4i}B_{3i}k_t\,(\theta_{t0i} - \theta_{s0i})\, e^{m_1 L} + \theta_{sLi} - \theta_{tLi}}{V_{si}V_{ti}(s + B_{3i} + B_{4i})(B_{3i} + B_{4i})(1 - e^{m_1 L})}$$

$$g_2 = B_{ti}k_t - \frac{B_{ti}B_{4i}k_t}{s + B_{3i} + B_{4i}} \frac{B_{3i}}{(B_{3i} + B_{4i})(1 - e^{m_1 L})} \frac{(\theta_{t0i} - \theta_{s0i})\, e^{m_1 L} + \theta_{sLi} - \theta_{tLi}}{V_{ti}^2}$$

$$h_1 = \frac{B_{si}B_{4i}B_{3i}k_t(\theta_{tLi} - \theta_{t0i} - \theta_{sLi} + \theta_{s0i})}{V_{si}V_{ti}(s + B_{3i} + B_{4i})(B_{3i} + B_{4i})(1 - e^{m_1 L})}$$

$$h_2 = \frac{\theta_{tLi} - \theta_{t0i}}{1 - e^{m_1 L}} \frac{m_1}{V_{ti}} + g_2 \frac{\theta_{tLi} - \theta_{t0i} - \theta_{sLi} + \theta_{s0i}}{(\theta_{t0i} - \theta_{s0i})\, e^{m_1 L} + \theta_{sLi} - \theta_{tLi}}$$

$$K_s = \frac{UP_t}{\rho_s A_s Cp_s} = K_{si}\left(1 + \frac{k_s V_s'}{V_{si}} + \frac{k_t V_t'}{V_{ti}}\right)$$

$$K_t = \frac{UP_t}{\rho_t A_t Cp_t} = K_{ti}\left(1 + \frac{k_s V_s'}{V_{si}} + \frac{k_t V_t'}{V_{ti}}\right)$$

$$m_2 = \frac{K_{si}}{V_{si}} - \frac{K_{ti}}{V_{ti}}$$

$$N_1 = \left(\frac{\theta_{sLi} - \theta_{s0i}}{e^{m_2 L} - 1}\right)\left(\frac{m_2}{V_{si}}\right)$$

$$N_2 = \left(\frac{\theta_{tLi} - \theta_{t0i}}{e^{m_2 L} - 1}\right)\left(\frac{m_2}{V_{ti}}\right)$$

$$Q_2 = \frac{K_{ti}K_t C}{V_{ti}}$$

$$R_2 = \frac{K_{ti}k_t D}{V_{ti}}$$

$$\alpha_1 = \frac{s + K_{si}}{V_{si}}$$

$$\alpha_2 = \frac{s + K_{ti}}{V_{ti}}$$

LITERATURE CITED

1. Edwards, Charles L., Ph.D. thesis, University of Wisconsin, Madison, Wisconsin (1958).
2. Gilliland E. R., L. A. Gould, and I. H. Rinard, "A Series Method for the Analysis of Plug Flow Process Dynamics, Part I," Mass. Inst. Technol., Cambridge, Massachusetts (1961).
3. Hempel, Arvid, *Trans. Am. Soc. Mech. Engrs.*, **82**, 244-251 (1961).
4. Koppel, Lowell B., *Ind. Eng. Chem. Fund.*, 1, No. 2, pp. 131-134 (1962).
5. Mozley, J. M., *Ind. Eng. Chem.*, **48**, 1035-1041 (1956).
6. Stermole, F. J., Ph.D. thesis, Iowa State University, Ames, Iowa (1963).
7. ———, and M. A. Larson, *Ind. Eng. Chem. Fund.*, **2**, 62-67 (1963).

Manuscript received August 28, 1963; revision received March 23, 1964; paper accepted March 25, 1964. Paper presented at A.I.Ch.E. Houston meeting.

Viscosity Correlation for Light Hydrocarbon Systems

A. L. LEE, K. E. STARLING, J. P. DOLAN, and R. T. ELLINGTON

Institute of Gas Technology, Chicago, Illinois

The needs of modern fluid processing and transmission and reservoir engineering for better information on fluid properties are well known. The authors and their associates have engaged in a series of studies to help meet these needs regarding data and prediction of hydrocarbon viscosities. These have included obtaining data on pure materials (*1, 2, 3, 4*) and mixtures (*5*) and efforts to use developments in modern molecular theory of fluids to obtain relationships for representing viscosity behavior (*6, 7*).

A semiempirical equation was quantitatively derived which represented the data on methane, ethane, propane, and *n*-butane including the continuity of states exhibited by the data. This paper reports the results of initial efforts to represent the viscosity behavior of binary light hydrocarbon mixtures.

EXPERIMENTAL

All the data cited above were obtained with the same absolute capillary tube viscometer. The data obtained with it have proved to be internally consistent and to agree well with those of other investigations. The instrument and its operation have been described in detail elsewhere (*5, 8*); its operating range is from ambient temprature to 400°F. and atmospheric pressure to 8,000 lb./sq. in. abs.

The primary data analyzed in this investigation are the methane data of Comings et al. (*9*), the ethane, propane, and *n*-butane data of Institute of Gas Technology (*1, 2, 4*), and the methane-*n*-butane binary mixture data of Dolan, Ellington, and Lee (*5*).

THEORY AND PREVIOUS WORK

The viscosity fields of ethane, propane, and *n*-butane were determined experimentally with sufficient detail that extensive correlative efforts were justified. The primary objective of these efforts was to achieve predictability of values of the same order of accuracy as the data (average error felt to be less than 0.5%) and to achieve the continuity of states exhibited by the data for the single-phase regions.

K. E. Starling is with Humble Oil Company, Houston, Texas. R. T. Ellington is with Sinclair Research, Inc., Tulsa, Oklahoma.

The modern theories of the general fluid indicate that the coefficient of viscosity should be expressed as the sum of two terms (*6, 7*)

$$\mu = \mu_K + \mu_\phi \tag{1}$$

The terms μ_K and μ_ϕ are usually referred to as the kinetic and intermolecular force contributions to viscosity, respectively. The first term arises from consideration of the transfer of momentum due to the free motion of the molecules between collisions. This is the only type of momentum transfer considered in simple kinetic theory, that is at low density. The second term arises from consideration of the transfer of momentum due to the action of intermolecular forces. Consideration of these forces is most important at high density.

Both the kinetic and intermolecular force contribution to viscosity are a function of temperature T and density ρ. In the dilute gas limit, where the only contribution to viscosity is by the thermal motion of the molecules, μ_K is a function of temperature only, and μ_ϕ vanishes. Thus the following conditions must be satisfied:

$$\lim_{\rho \to 0} \mu_K (T, \rho) = \mu_o (T) \tag{2}$$

$$\lim_{\rho \to 0} \mu_\phi (T, \rho) = 0 \tag{3}$$

Accurate expressions for μ_K and μ_ϕ for high density have not been developed. However because μ_K does not differ greatly from μ_o even for moderate densities, it usually may be replaced by μ_o in Equation (1) for semiempirical analysis.

Starling and Ellington (*7*) developed several semiempirical equations, based in varying degrees on the theory of viscosity due to Born and Green (*10*). The correlation presented here is derived from their final equation. The following expression for viscosity

$$\mu = \mu_o + K_1 \rho^{5/3} \exp\left[\frac{K_2}{T} \rho^2\right] \tag{4}$$

which Starling and Ellington derived directly from the Born and Green theory is presented here. For theoretical